



## Sensitivity and selectivity determination of bisphenol A using SWCNT–CD conjugate modified glassy carbon electrode

Yong Gao<sup>a</sup>, Yu Cao<sup>a</sup>, Duanguang Yang<sup>a</sup>, Xujun Luo<sup>a</sup>, Yiming Tang<sup>a</sup>, Huaming Li<sup>a,b,\*</sup>

<sup>a</sup> College of Chemistry, Xiangtan University, Xiangtan 411105, Hunan Province, PR China

<sup>b</sup> Key Laboratory of Polymeric Materials & Application Technology of Hunan Province, Key Laboratory of Advanced Functional Polymeric Materials of College of Hunan Province, and Key Lab of Environment-friendly Chemistry and Application in Ministry of Education, Xiangtan University, Xiangtan 411105, Hunan Province, PR China

### ARTICLE INFO

#### Article history:

Received 22 September 2011  
Received in revised form 18 October 2011  
Accepted 22 October 2011  
Available online 29 October 2011

#### Keywords:

Bisphenol A  
Single-walled carbon nanotubes  
β-Cyclodextrin  
Electrochemistry  
Modified electrode

### ABSTRACT

In this study, we demonstrated a highly sensitive electrochemical sensor for the determination of bisphenol A (BPA) in aqueous solution by using single-walled carbon nanotubes (SWCNTs)/β-cyclodextrin (β-CD) conjugate (SWCNT–CD) modified glassy carbon electrode (GCE). The cyclic voltammetry results show that the modified GCE exhibits strong catalytic activity toward the oxidation of BPA with a well-defined cyclic voltammetric peak at 0.543 V. The response current exhibits a linear range between 10.8 nM and 18.5 μM with a high sensitivity (1256 μA mM<sup>-1</sup>). The detection limit of BPA is 1.0 nM (S/N = 3). The enhanced performance of the fabricated sensor can be attributed to the combination of the excellent electrocatalytic properties of SWCNTs and the molecular recognition ability of β-CD. The sensor was successfully applied to determine BPA leached from real plastic samples with good recovery, ranging from 95% to 103%.

© 2011 Elsevier B.V. All rights reserved.

### 1. Introduction

Bisphenol A (BPA, 2,2'-bis(4-hydroxyphenyl)propane) is an endocrine disruptor, which can mimic the body's own hormones and may lead to negative health effects [1]. The first study of health effects on humans associated with BPA exposure was reported in 2008 by Lang et al. [2], in which they found that higher BPA levels were significantly associated with heart disease, coronary heart disease, diabetes, and abnormally high levels of certain liver enzymes. A later study at Tufts University Medical School concluded that BPA might increase cancer risk [3]. In recent years, the concern over the effect of BPA on humans was heightened by the fact that infants and children are estimated to have the highest daily intake of BPA, because BPA is the key monomer in the production of polycarbonate (PC) plastics, which are widely used to make a variety of common products including baby bottles and water bottles, medical and dental devices, eyeglass lenses, and household electronics. Additionally, BPA-based epoxy resins are usually used as coatings on the inside of almost all food and beverage cans. Unfortunately,

BPA has been known to be leached from these plastics, especially those that are cleaned with harsh detergents or those that contain acidic or high-temperature liquids. A recent Health Canada study found that the majority of canned soft drinks it tested had low, but measurable levels of BPA [4]. Therefore, in September 2010, Canada became the first country to declare BPA as a toxic substance and banned the use of BPA in baby bottles [5]. So, the development of new methods for the determination of BPA at trace concentrations has become one of the most attractive subjects of investigation in analytical chemistry because of the practical applications.

Various analytic methods have been developed and used for the determination of BPA. Such methods include liquid chromatography (LC), liquid chromatography–mass spectrometry (LC–MS), gas chromatography–mass spectrometry (GC–MS), liquid chromatography with electrochemical detector (LC–ECD), chemiluminescence, enzyme-linked immunosorbent assay (ELISA), and electrochemical techniques [6–17]. Among them, electrochemical method has great potential for environmental monitoring because of its inherent advantages such as fast response speed, ease of miniaturization, low cost, timesaving, high sensitivity, excellent selectivity, and in vivo real-time determination. However, a major obstacle encountered in the determination of BPA by electrochemical method is the relatively high overpotential together with poor reproducibility although BPA can be oxidized at electrode surface due to containing phenolic hydroxyl groups [18]. Additionally, bare electrode often suffers from a fouling effect, which causes rather poor selectivity and sensitivity [19]. An effective way to

\* Corresponding author at: Key Laboratory of Polymeric Materials & Application Technology of Hunan Province, Key Laboratory of Advanced Functional Polymeric Materials of College of Hunan Province, and Key Lab of Environment-friendly Chemistry and Application in Ministry of Education, Xiangtan University, Xiangtan 411105, Hunan Province, PR China. Tel.: +86 731 58298572; fax: +86 731 58293264.

E-mail address: [lihuaming@xtu.edu.cn](mailto:lihuaming@xtu.edu.cn) (H. Li).

overcome these barriers is electrode modification. Modified electrode is capable of reducing the overvoltage and overcoming the slow kinetics of many electrode processes. Enzyme [17], functionalized polymer [20], nanoparticles [21], and carbon materials, especially one-dimensional carbons, such as carbon nanotubes (CNTs) [22] and carbon fibers [23], have been successfully used to modify bare electrode.

Owing to their high electrical catalytic properties, high chemical stability and extremely high mechanical strength, CNTs have been focused on the field of modification of electrode surface [24,25]. The CNT modified electrode has shown superior performance due to its ability of promoting electron transfer reactions with electroactive species present in solution [26]. However, the intrinsic van der Waals interactions between the pristine tubes make CNT bundles in scale and insoluble in routine solvents [27]. Therefore, CNT bundles are required to disperse in solvent prior to the electrode modification. Several approaches to the functionalization of CNTs, including noncovalent exohedral interactions [24] and covalent sidewall coupling reactions [25], have been developed to disperse CNTs. Recently, independent research groups in China [28,29] have reported the determination of BPA by electrochemical method using multiwalled CNT (MWCNT) modified electrode with a detection limit of 7.5 and 5.0 nM, respectively. However, it is still a challenge to fabricate new electrochemical sensors based on familiar carbon materials with higher sensitivity through exfoliation of the CNT bundles into small bundles or individual nanotubes, together with the incorporation of molecular recognition sites onto the surface of CNTs.

Cyclodextrins (CDs) are cyclic oligosaccharides with D-(+)-glucose as the repeating unit coupled by 1,4- $\alpha$ -linkages [30].  $\alpha$ -,  $\beta$ -, and  $\gamma$ -CDs are commonly available forms which consist of 6, 7, and 8 glucose units, respectively. The most characteristic property of CDs is their remarkable ability to form inclusion complexes with a wide variety of guest molecules due to their different cavity sizes [31–33]. This property enables CD modified electrode to improve selectivity. Accumulating properties of  $\beta$ -CD self-assembled on gold electrode surface were demonstrated with respect to BPA by using cyclic voltammetry [34,35]. Up to now, the selectivity of CDs has not been thoroughly realized for CD-modified electrodes. Nevertheless, CDs play an important and undisputed role among the electrode modifiers, and electrodes with attached CDs have been successfully utilized for the solution of many specific electrochemical and electroanalytical tasks.

In the present work, single-walled CNTs (SWCNTs) were firstly functionalized with  $\beta$ -CD (SWCNT-CD). Consequently, glassy carbon electrode (GCE) was coated with SWCNT-CD film. The modified electrode, SWCNT-CD/GCE, was further used to determine BPA by using cyclic voltammetry and amperometry. To the best of our knowledge, there is no report on the modification of GCE with SWCNT-CD conjugate to detect BPA. The modified GCE will combine the electrocatalytic properties of SWCNTs and the selective inclusion property of  $\beta$ -CD, which exhibits an attractive ability for highly sensitive determination of BPA in real samples. The sensitivity, linear range, limits of detection and stability of the prepared electrochemical sensor in the detection of BPA were also investigated.

## 2. Experiments

### 2.1. Reagents and apparatus

SWCNTs with the external diameter less than 2 nm and length 5–15  $\mu$ m were obtained from Shenzhen Nanotech Port Co. Ltd. (Shenzhen, China), which was prepared by the chemical

vapor deposition (CVD) method. HDA- $\beta$ -CD (mono-6-deoxy-6-hexanediamino- $\beta$ -CD) was prepared through two successive reactions according to the method reported elsewhere [36,37]. BPA was purchased from Aldrich. 1.0 mM BPA stock solution was prepared with anhydrous ethanol and kept in darkness at 4 °C. A series of phosphate buffer solutions (PBSs) with different pH were prepared by mixing the solutions of 0.1 M  $\text{NaH}_2\text{PO}_4$  and 0.1 M  $\text{Na}_2\text{HPO}_4$ , and then adjusting the pH with HCl or NaOH. All other reagents were analytical reagent grade and used as received without further purification. All the solutions were prepared with doubly distilled water. Thermogravimetric analysis (TGA) was carried out on a STA 449C instrument under a flowing nitrogen atmosphere. Transmission electron microscopy (TEM) analysis was performed on a JEOL JEM-3010 electron microscope.

Electrochemical experiments were performed with CHI630C electrochemical workstation (Shanghai Chenhua Co., China) with a conventional three-electrode cell. A bare GCE or modified GCE was used as working electrode. A saturated calomel electrode and a platinum wire electrode were used as reference electrode and auxiliary electrode, respectively. The pH measurements were carried out on pHs-3C exact digital pH meter (Shanghai Rex Co. Ltd., China). All the measurements were carried out at room temperature.

### 2.2. Preparation of SWCNT-CD

The synthesis of SWCNT-CD was performed by a two-step process. Firstly, a round-bottom flask was charged with 200 mg of SWCNTs and cooled in an ice water bath. Then, 20 mL of oxidant (concentrated  $\text{H}_2\text{SO}_4/\text{HNO}_3$ , 3/1, v/v) was slowly added. The mixture of SWCNTs and the acid was subjected to sonication at 0 °C for 30 min. The flask was then immersed into an oil bath at 20 °C and stirred for 20 h. The dispersion was then carefully poured into 1000 mL of deionized water. The black slurry was vacuum filtered on a 0.22  $\mu$ m Teflon membrane, resulting in the formation of a SWCNT filter cake. The SWCNTs were then subjected to dispersion by sonication and rinsed with deionized water until the pH value of the filtrate was neutral. The resultant SWCNT-COOH was dried under vacuum. TGA result indicates that the carboxylic acid incorporation density is about 2.08 mmol per gram of neat SWCNTs.

Secondly, 20 mg of SWCNT-COOH was treated with excess  $\text{SOCl}_2$  (30 mL, 0.42 mol) at 65 °C for 24 h. The residual  $\text{SOCl}_2$  was removed by reduced pressure distillation, giving acyl chloride-functionalized SWCNTs (SWCNT-COCl). The as-produced SWCNT-COCl was then dispersed in 20 mL of anhydrous DMF and immediately reacted with HDA- $\beta$ -CD (5.00 g, 4.00 mmol) for 24 h at 65 °C. After repeated washing with methanol (5  $\times$  60 mL) and filtration, the resulting SWCNT-CD was dried overnight under vacuum.

### 2.3. Preparation of SWCNT-CD/GCE

The GCE was polished sequentially with sandpaper, and 0.05  $\mu$ m alumina slurry on polishing cloth to produce a mirror-like surface. It was then sonicated for 1.0 min in  $\text{HNO}_3$ /water (1/1, v/v), ethanol/water (1/1, v/v) and doubly distilled water in an ultrasonic bath, respectively. Subsequently, it was dried under IR lamp. For preparation of modified electrode, 1.0 mg mL<sup>-1</sup> of SWCNT-CD aqueous suspension was prepared with doubly distilled water, and then 10  $\mu$ L of the suspension was deposited on the fresh treated GCE surface with a pipette. After the solvent evaporated, the electrode surface was thoroughly rinsed with doubly distilled water and dried under ambient condition. For comparison, SWCNT-COOH modified GCE (SWCNT-COOH/GCE) and the blended mixture of SWCNT-COOH and CD modified GCE (SWCNT-COOH/CD/GCE) were fabricated with similar procedures.

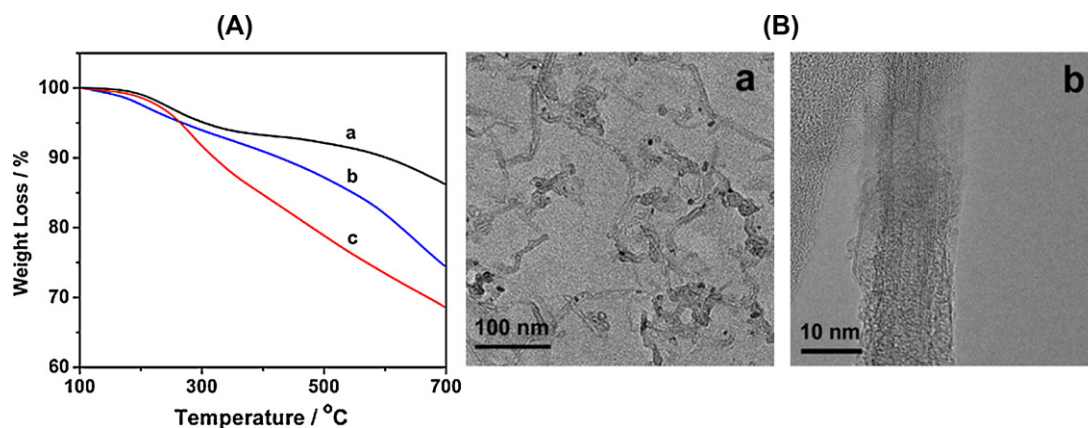


**Fig. 1.** (A) TGA plots of (a) pristine SWCNTs, (b) SWCNT-COOH, and (c) SWCNT-CD, acquired under nitrogen at a ramp of  $10^{\circ}\text{C min}^{-1}$ . (B) Representative TEM images of SWCNT-CD.

### 3. Results and discussion

#### 3.1. Electrode modification

In the present study, GCE was modified with SWCNT-CD conjugate prior to use. The SWCNT-CD conjugate was prepared as described in Section 2. The content of  $\beta$ -CD grafted on the surface of SWCNTs was analyzed by TGA and the result is shown in Fig. 1A. For comparison, the TGA plots of pristine SWCNTs and oxidized SWCNTs are also shown in Fig. 1A. Using the mass loss of SWCNT-COOH at  $500^{\circ}\text{C}$  as the reference, the mass loss of SWCNT-CD is about 7.5 wt% at  $500^{\circ}\text{C}$ , indicating that about 13.8% of the available carboxylic acid groups have reacted with  $\beta$ -CD. The morphology of SWCNT-CD was also imaged by a high resolution TEM as depicted in Fig. 1B. Based on the observation, it is clear that the SWCNT-CD can be well dispersed in water, and small bundles, even individual tubes were observed. The  $\beta$ -CD was immobilized on the tips as well as sidewalls of the SWCNTs. Meanwhile, the grafted  $\beta$ -CD components were not uniformly coated on the SWCNT surface.

#### 3.2. Electrochemical performance of SWCNT-CD/GCE

The electron transfer properties of the electrode after different surface modifications were characterized by electrochemical impedance spectroscopy (EIS). Generally, the linear part in the EIS represents the diffusion-limited process, while the semicircle portion corresponds to the electron transfer-limited process. The electron transfer resistance ( $R_{et}$ ) at electrode surface is equal to the semicircle diameter [38]. Fig. 2 shows Nyquist diagrams of different electrodes in  $5.0\text{ mM } [\text{Fe}(\text{CN})_6]^{3-/4-}$  solution containing  $0.1\text{ M KCl}$ . As can be seen, the  $R_{et}$  of the bare GCE is  $1400\ \Omega$  (curve a), indicating a huge interface electron transfer resistance. The  $R_{et}$  value decreases after the bare electrode was modified with the mixture of SWCNT-COOH and  $\beta$ -CD ( $500\ \Omega$ , curve c), suggesting that the SWCNTs can improve the conductivity and the electron transfer process [39]. However, the  $\beta$ -CD layer absorbed on the electrode surface still hinders the electron transfer from the redox probe of  $[\text{Fe}(\text{CN})_6]^{3-/4-}$  to the electrode surface. For the SWCNT-CD modified GCE, the  $R_{et}$  drastically decreases to  $150\ \Omega$  (curve d). Compared with bare GCE or even the SWCNT-COOH/CD/GCE surface, the SWCNT-CD film greatly improves the conductivity and the electron transfer process. Interestingly, a nearly straight line is observed when SWCNT-COOH was immobilized on GCE surface (curve b), indicating a very small interfacial electron transfer resistance. These results also demonstrated that SWCNT-CD was successfully immobilized on the GCE surface.

Cyclic voltammograms of the bare GCE and modified GCEs in PBS (pH 8.0) with  $10\ \mu\text{M}$  BPA are shown in Fig. 3. It can be seen that no peaks are observed for the bare GCE (curve a). However, a well-defined oxidation peak is observed during the sweep from 0.30 to 0.90 V at the modified GCEs, while no corresponding reduction peak is observed, indicating that the electrode response of BPA

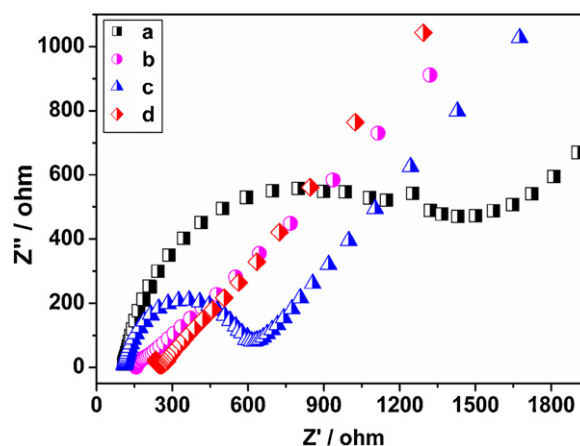


**Fig. 2.** Nyquist plots of different electrodes in  $5.0\text{ mM } [\text{Fe}(\text{CN})_6]^{3-/4-}$  (1/1) solution containing  $0.1\text{ M KCl}$ , (a) GCE, (b) SWCNT-COOH/GCE, (c) SWCNT-COOH/CD/GCE, and (d) SWCNT-CD/GCE.

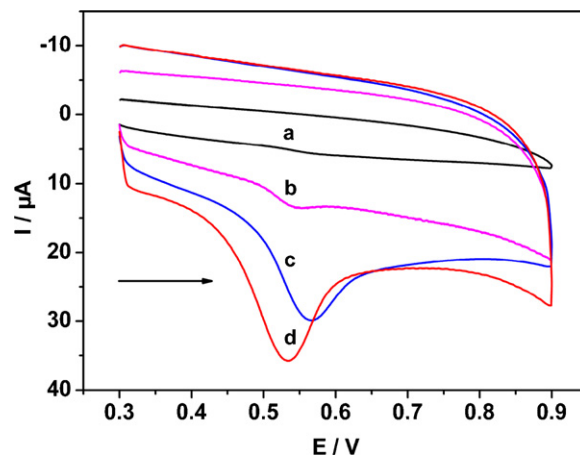


**Fig. 3.** Cyclic voltammograms of (a) GCE, (b) SWCNT-COOH/GCE, (c) SWCNT-COOH/CD/GCE, and (d) SWCNT-CD/GCE in  $0.1\text{ M PBS}$  (pH 8.0) containing  $10\ \mu\text{M}$  BPA. Scan rate:  $100\text{ mV s}^{-1}$ . The arrow indicates scanning direction.

is a typical irreversible electrode reaction. It is worth noting that the oxidation current of BPA at SWCNT-COOH/CD/GCE increases when compared with SWCNT-COOH/GCE, which can be attributed to the accumulation properties of  $\beta$ -CD due to the host-guest interaction between  $\beta$ -CD and BPA [35]. The oxidation current further increases and the oxidation potential shifts more negatively when SWCNT-CD was immobilized on the surface of GCE. This result can be attributed to the synergetic activity of SWCNTs and  $\beta$ -CD, in which the negative potential shift indicates the significant electrocatalytic activities of the SWCNTs due to the residual metal as well as metal oxide impurities [40–42], and the increase in current can be ascribed mainly to the surface accumulation ability of the grafted  $\beta$ -CD. Therefore, covalently bonded  $\beta$ -CD onto the surface of SWCNTs plays an important role in electrode modification. Nevertheless, the electrostatic repulsion between the SWCNT-COOH and negatively charged BPA would result in the oxidation reaction deceleration in the case of SWCNT-COOH/GCE. Meanwhile, the aggregates of  $\beta$ -CD are formed by assembly and a mixture of aggregates of different sizes may be present in the suspension, which may suppress the accumulation ability of  $\beta$ -CD, and thus decrease the sensitivity for BPA as in the case of SWCNT-COOH/CD/GCE. Thus, the electrode coated with SWCNT-CD conjugate can increase the conductive area, and enhance the electron transfer rate between BPA and the electrode surface.

The oxidation peak potential of BPA at SWCNT-CD/GCE (0.543 V) was smaller than some of previous reports in near neutral pH conditions, such as Si/boron-doped electrode (1.2 V, vs. SCE) [43], carbon fiber electrode (0.75 V, vs. Ag/AgCl) [44], MWCNT/GCE (0.59 V, vs. Ag/AgCl) [22], and MWCNT-COOH/GCE (0.55 V, vs. SCE) [29]. Therefore, a substantial decrease in oxidation overpotential has been achieved in the present study with SWCNT-CD/GCE. The difference of oxidation potential of BPA might be attributed to the electrolyte, matrix electrode, modification procedure, and modification materials.

### 3.3. Optimization of experimental conditions

The aim of this work is to establish a simple and sensitive electrochemical method for the determination of BPA. As mentioned above, the oxidation peak of BPA is remarkably heightened at SWCNT-CD/GCE vs. bare GCE, giving an enhanced sensitivity for BPA determination. However, optimization of experimental conditions for the determination of BPA is of critical importance. Hence, a systematic investigation of a number of variables related to cyclic voltammograms, such as the amounts of SWCNT-CD loading, solution pH, scanning rate, and accumulation potential as well as time has been conducted.

Fig. 4 shows the effect of the amount of SWCNT-CD suspension that was cast onto the GCE surface on the oxidation current of 10  $\mu$ M BPA in 0.1 M PBS (pH 8.0). Clearly, the oxidation peak current of BPA is dependent on the amounts of SWCNT-CD suspension that was cast onto the GCE surface. The oxidation peak current of BPA increases significantly with the amount of SWCNT-CD suspension increasing from 2.0 to 8.0  $\mu$ L, while the peak current keeps almost stable from 8.0 to 10  $\mu$ L. However, when the amount of the suspension exceeds 10  $\mu$ L, the peak current decreased instead. This is due probably to the limited mass transport of BPA inside a thicker film. Considering that water evaporation required a long time, we chose 10  $\mu$ L of SWCNT-CD suspension to modify the electrode.

Next, the effect of PBS pH on the electrochemical response of the SWCNT-CD/GCE toward the determination of the BPA was studied by cyclic voltammetry. The variations of peak current as well as the oxidation peak potential with respect to the change of the electrolyte in the pH range from 5.0 to 9.0 are shown in Fig. 5. It can be seen in Fig. 5B that the peak current increases slowly with the increasing of the solution pH from 5.0 to 8.0, and then decreases

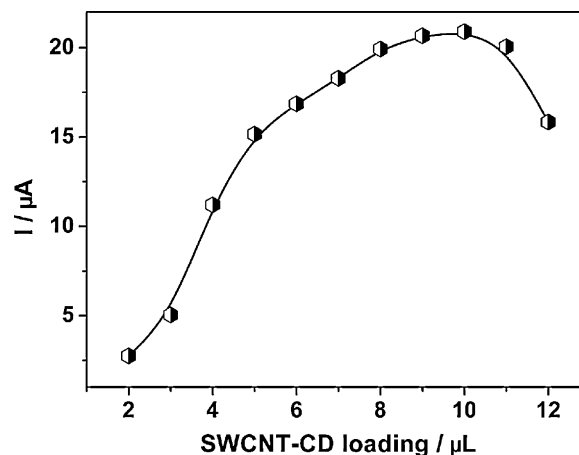


Fig. 4. Influence of the amount of SWCNT-CD suspension on the oxidation peak current of 10  $\mu$ M BPA. Cyclic voltammogram measurements were performed in 0.1 M PBS (pH 8.0). Scan rate: 100  $\text{mV s}^{-1}$ .

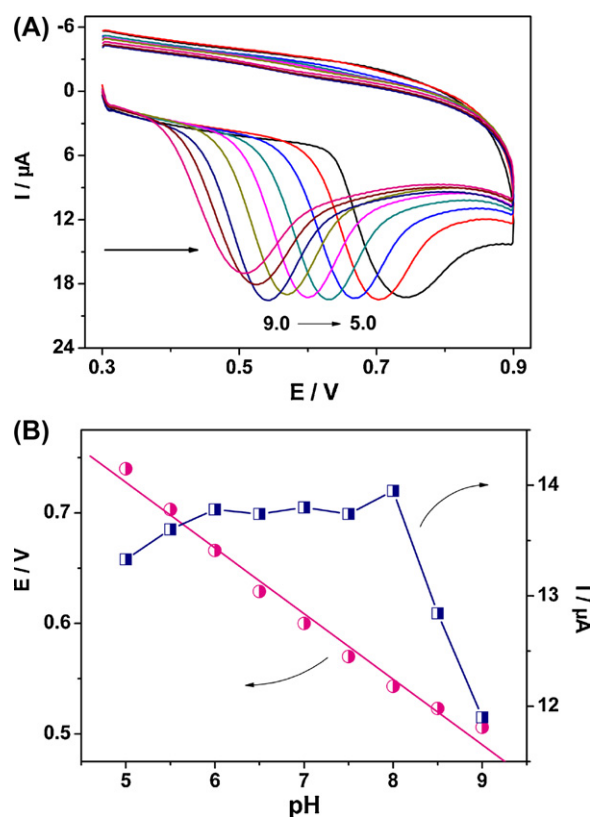


Fig. 5. (A) Cyclic voltammograms of SWCNT-CD/GCE to 1.0  $\mu$ M BPA in 0.1 M PBS of different pH: 5.0, 5.5, 6.0, 6.5, 7.0, 7.5, 8.0, 8.5, and 9.0. (B) Effects of pH on the peak current and potential. Scan rate: 100  $\text{mV s}^{-1}$ . The arrow indicates scanning direction.

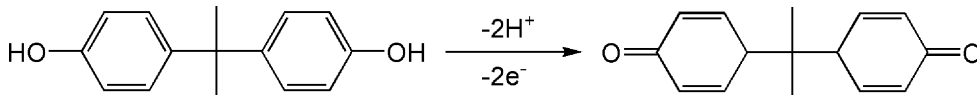
with a further increase of pH, showing that protons have taken part in the electrode reaction process [45]. As the pH increases beyond 8.0, the residual carboxylic acid groups on the surface of SWCNTs are deprotonated to a large extent and therefore exist as anions, resulting in mutual repulsion between the acidic anions and the negatively charged BPA, leading to decrease of the current response, since BPA can form phenolic oxide anion in alkaline solution [46]. Considering the sensitivity of the determination of BPA, a pH of 8.0 was chosen for the subsequent analytical experiments. The relationship between the oxidation peak potential ( $E_{pa}$ ) and pH is also shown in Fig. 5B. It is found that the value of peak potential at SWCNT-CD/GCE shifted to more negative potential

with the increase of pH from 5.0 to 9.0, and that it obeys the following equation:  $E_{pa}$  (V) =  $-0.059\text{pH} + 1.024$  ( $R = 0.993$ ). A shift of typically 59 mV per pH unit is approximately close to the theoretical value of  $57.6 \text{ mV pH}^{-1}$  [45], indicating that the electron transfer is accompanied by an equal number of protons in electrode reaction.

Cyclic voltammograms of the fabricated SWCNT-CD/GCE at different scan rates were also recorded (Fig. 6A). It can be seen that the peak currents ( $I_{pa}$ ) increase linearly with the scan rate ( $\nu$ ) in the range of 30–150  $\text{mV s}^{-1}$  (Fig. 6B), indicating that the oxidation of BPA at SWCNT-CD/GCE is a process controlled by electron transfer [45]. And the linear regression equation can be expressed as  $I_{pa}$  ( $\mu\text{A}$ ) =  $0.167\nu$  ( $\text{mV s}^{-1}$ ) +  $3.845$  ( $R = 0.997$ ). Similarly, a linear relationship between  $E_{pa}$  and Napierian logarithm of  $\nu$  ( $\ln \nu$ ) is also observed in the range of 30–400  $\text{mV s}^{-1}$  (Fig. 6C). The equation can be expressed as  $E_{pa} = 0.033 \ln \nu + 0.400$  ( $R = 0.996$ ). As for an electron transfer controlled and totally irreversible electrode process,  $E_{pa}$  is defined by the following equation [47]:

$$E_{pa} = E^0 + \left(\frac{RT}{\alpha nF}\right) \ln \left(\frac{RTk^0}{\alpha nF}\right) + \left(\frac{RT}{\alpha nF}\right) \ln \nu \quad (1)$$

where  $\alpha$  is transfer coefficient,  $k^0$  is standard rate constant of the reaction,  $n$  is electron transfer number involved in rate-determining step,  $\nu$  is scanning rate,  $E^0$  is formal redox potential,  $R$  is the gas constant,  $T$  is the absolute temperature, and  $F$  is the Faraday constant. According to the linear correlation of  $E_{pa}$  vs.  $\ln \nu$  as mentioned above, the slope of the line is equal to  $RT/\alpha nF$ , therefore  $\alpha n$  is calculated to be 1.29. Generally,  $\alpha$  is assumed to be 0.5 in totally irreversible electrode process [45], so the electron transfer number ( $n$ ) is around 2. Considering that the number of electron and proton involved in the oxidation process of BPA is equal as demonstrated in the pH-dependent electrochemical response, the electrooxidation of BPA at SWCNT-CD/GCE is a two-electron and two-proton process, which can be illustrated as follows:



The standard heterogeneous rate constant ( $k_s$ ) for totally irreversible oxidation of BPA at the modified electrode is calculated based on Velasco equation [48]:

$$k_s = 2.415 \exp\left(-\frac{0.02F}{RT}\right) D^{1/2} (E_{pa} - E_{pa/2})^{-1/2} \nu^{1/2} \quad (2)$$

where  $E_{pa/2}$  represents the potential at which  $I = I_{pa}/2$  in linear sweep voltammetry,  $D$  is diffusion coefficient, other symbols have their usual meanings.  $D$  can be determined by chronocoulometry according to Anson equation [49]:

$$Q = 2nFAc \left(\frac{Dt}{\pi}\right)^{1/2} + Q_{dl} + Q_{ads} \quad (3)$$

where  $A$  is surface area of working electrode,  $c$  is concentration of substrate,  $Q_{dl}$  is double layer charge which can be eliminated by background subtraction, and  $Q_{ads}$  is Faradaic charge. Other symbols have their usual meanings. The experiment was firstly carried out in 0.1 mM  $\text{K}_3[\text{Fe}(\text{CN})_6]$  solution containing 1.0 mM KCl, where the standard diffusion coefficient ( $D_0$ ) of  $\text{K}_3[\text{Fe}(\text{CN})_6]$  at  $25^\circ\text{C}$  is  $7.6 \times 10^{-6} \text{ cm}^2 \text{ s}^{-1}$  [45]. According to the experiment results as shown in Fig. 7A,  $A$  is calculated to be  $0.021 \text{ cm}^2$  and  $0.36 \text{ cm}^2$  for GCE and SWCNT-CD/GCE, respectively. These results indicate that the electrode effective surface area increases obviously after electrode modification. The surface can therefore be thought of as a porous layer in which pockets of solution are trapped in between multiple layers of nanotubes [50,51]. The chronocoulometry experiments were then carried out at SWCNT-CD/GCE in 0.1 M PBS (pH 8.0) in the absence and presence of 0.25 mM BPA. As

shown in Fig. 7B, the plot of  $Q$  against  $t^{1/2}$  shows a linear relationship after background subtraction. The slope is  $1.26 \times 10^{-4} \text{ C s}^{-1/2}$  and the intercept ( $Q_{ads}$ ) is  $1.10 \times 10^{-5} \text{ C}$ . As  $n=2$ ,  $A=0.36 \text{ cm}^2$ , and  $c=0.25 \text{ mM}$ ,  $D$  is calculated to be  $4.10 \times 10^{-5} \text{ cm}^2 \text{ s}^{-1}$  at  $25^\circ\text{C}$ . According to the equation  $Q_{ads} = nFA\Gamma_s$ , the adsorption capacity,  $\Gamma_s$ , can be obtained as  $1.58 \times 10^{-10} \text{ mol cm}^{-2}$ . Similarly, the  $k_s$  of BPA is thus calculated to be about  $0.011 \text{ cm s}^{-1}$ . This  $k_s$  is higher than those of previously reported CNT-based sensors. Such sensors include CNT powder microelectrode ( $1.90 \times 10^{-3} \text{ cm s}^{-1}$ ) [52], MWCNTs/GCE ( $3.62 \times 10^{-3} \text{ cm s}^{-1}$ ) [53], and MWCNT-COOH/GCE ( $3.83 \times 10^{-3} \text{ cm s}^{-1}$ ) [54], but close to Au-MWCNTs/GCE ( $0.013 \text{ cm s}^{-1}$ ) [55]. These results suggest that the SWCNT-CD/GCE provide fast electron transfer between BPA and the surface of electrode.

Finally, the influences of accumulation potential as well as time on the oxidation peak current obtained at the SWCNT-CD/GCE were investigated, since the accumulation step is usually a simple and effective way to enhance the sensitivity. The oxidation peak current of 10  $\mu\text{M}$  BPA carried in 0.1 M PBS (pH 8.0) was compared at different potentials. The highest oxidation peak current is achieved at  $-0.2 \text{ V}$  (Fig. 8A). The influence of the accumulation time on the oxidation peak current of BPA was also tested. The oxidation peak current increases greatly within the first 150 s and then levels off (Fig. 8B), suggesting that the accumulation of BPA at SWCNT-CD modified GCE rapidly reached saturation. Thus, the accumulation step in the experiments was performed at  $-0.2 \text{ V}$  for 150 s.

## 4. Analytical utility

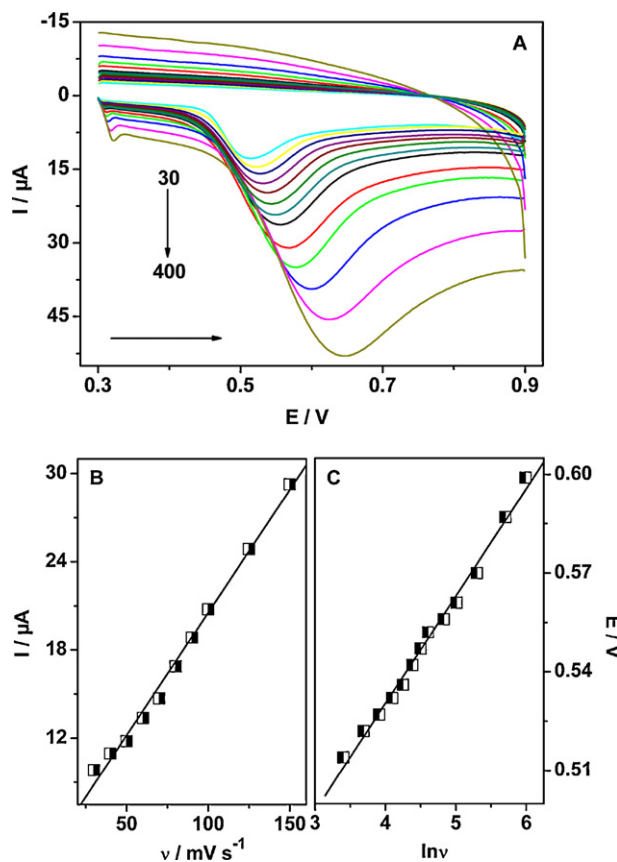
### 4.1. Calibration curve, linear range, and detection limit

Fig. 9 shows a typical current–time plot of SWCNT-CD/GCE under optimum experimental conditions after successive addition

of BPA, with concentrations ranging from 5.4 nM to 21.2  $\mu\text{M}$ , to 0.1 M PBS (pH 8.0) under magnetic stirring. The modified electrode can achieve the steady-state current within 5 s, which is a very rapid response to the change of BPA concentrations. As shown in Fig. 9B, the current linearly increased with the increase in BPA concentration ranging from 10.8 nM to 18.5  $\mu\text{M}$  with a correlation coefficient ( $R$ ) of 0.999 and a high sensitivity of about  $1256 \mu\text{A mM}^{-1}$ . The linear regression equation can be expressed as  $I$  ( $\mu\text{A}$ ) =  $1.256c$  ( $\mu\text{M}$ ) –  $0.922$ . The detection limit is estimated to be 1.0 nM at a ratio of signal to noise of 3, which is lower than that reported previously [14–17,22,28,29]. The enhanced performance of SWCNT-CD/GCE can be attributed to the combination of the excellent electrocatalytic properties of debundled SWCNTs and the inclusion ability of  $\beta$ -CD to BPA. Therefore, the SWCNT-CD/GCE can be served as a BPA sensor although the peak current tends to level off at higher BPA concentrations as shown in Fig. 9B, due to the saturation of active sites at the surface of electrode.

### 4.2. Reproducibility, stability and interference of SWCNT-CD/GCE

In order to prove the precision and practicability of the proposed method, the reproducibility and storage stability of the SWCNT-CD/GCE were investigated by cyclic voltammetry. The relative standard deviation of the modified electrode response to 10  $\mu\text{M}$  BPA is 2.2% after twenty successive measurements with the same modified electrode, showing excellent reproducibility of SWCNT-CD/GCE. As a further demonstration of the stability, the



**Fig. 6.** (A) Cyclic voltammograms of SWCNT-CD/GCE in 0.1 M PBS containing 10  $\mu\text{M}$  BPA at various scan rates: 30, 40, 50, 60, 70, 80, 90, 100, 125, 150, 200, 300, and 400  $\text{mV s}^{-1}$ . (B) The plot of peak current vs. scan rate. (C) The relationship between the peak potential ( $E_{pa}$ ) and the natural logarithm of scan rate ( $\ln v$ ). The arrow indicates scanning direction.

modified electrode was also investigated by measuring the current response of 10  $\mu\text{M}$  BPA. Before measurements, the electrode was stored at 4 °C in a refrigerator for 15 days. The current retained 95% of its original response. However, the current response decreased to 88% after prolonging the storage time to 30 days under the same conditions. The phenomenon indicated the good stability of SWCNT-CD/GCE.

Under optimal conditions, the interference test was performed in the presence of 100-fold concentration of phenol, 4-isopropylphenol, hydroquinone, pyrocatechol, hydroxyphenol, 4-nitrophenol, 2,4-dinitrophenol, ethanol,  $\text{Cu}^{2+}$ ,  $\text{Ca}^{2+}$ ,  $\text{Fe}^{3+}$ ,  $\text{Pb}^{2+}$ ,  $\text{Mg}^{2+}$ ,  $\text{Al}^{3+}$ ,  $\text{Zn}^{2+}$ ,  $\text{Br}^-$ ,  $\text{SO}_4^{2-}$ ,  $\text{NO}_3^-$ . The results indicate that they have no influence on the signals of 10  $\mu\text{M}$  BPA with deviation below 5.0%. Due to the excellent reproducibility, stability and the result of interference tests, SWCNT-CD/GCE can be used in practical analytical applications.

#### 4.3. Practical application

In order to evaluate the performance of SWCNT-CD/GCE in practical analytical applications, the determination of BPA in the real samples (such as PC baby bottle, PC water bottle, and poly(vinyl chloride) (PVC) bottle) was carried out via a recovery study according to the above-described analytical procedure. All the samples were collected from the disposal sites. The samples were pre-cleaned in an ultrasonic tub with acetone, rinsed successively with alcohol, doubly distilled water, and then dried. After being cut into small pieces, 1.0 g of plastic sample and 30 mL of doubly distilled water were added into a flask fitted with a condenser. The flask

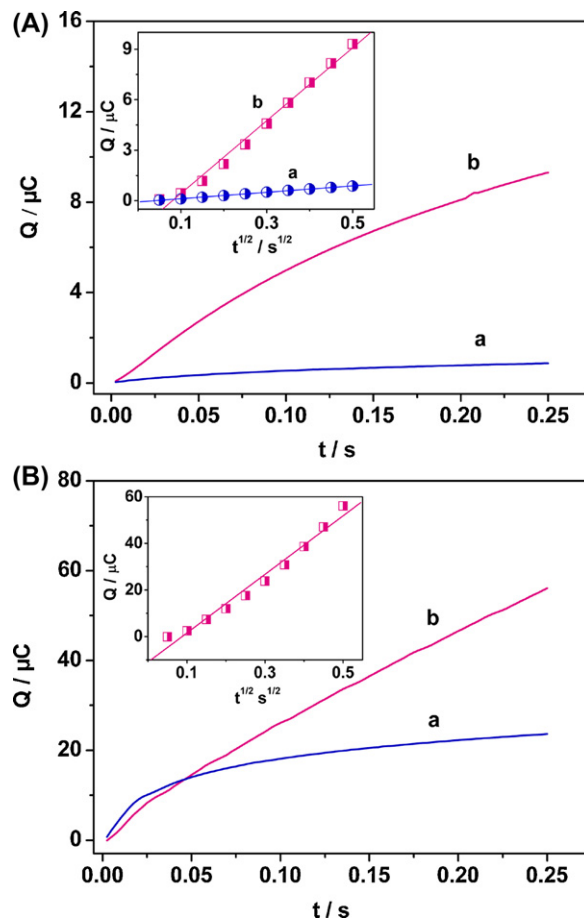


**Fig. 7.** (A) Plot of  $Q-t$  curves of (a) GCE, and (b) SWCNT-CD/GCE in 0.1 mM  $\text{K}_3[\text{Fe}(\text{CN})_6]$  containing 1.0 M KCl. Inset: plot of  $Q-t^{1/2}$  curves on (a) GCE, and (b) SWCNT-CD/GCE. (B) Plot of  $Q-t$  curves of the modified electrode in 0.1 M PBS (pH 8.0) (a) in the absence, and (b) presence of 0.25 mM BPA. Inset: plot of  $Q-t^{1/2}$  curve on SWCNT-CD/GCE.

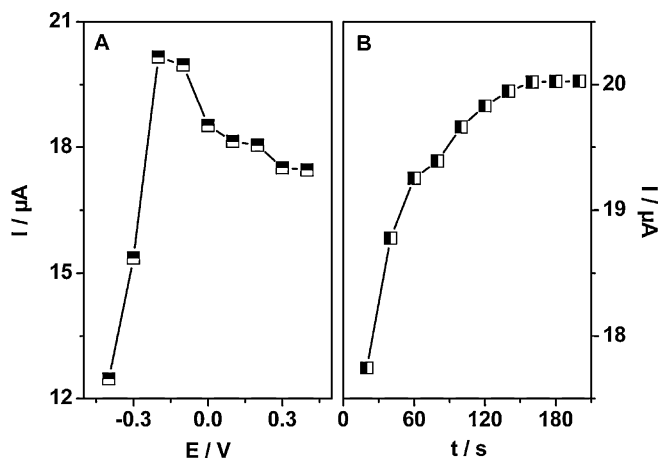


**Fig. 8.** Effect of (A) accumulation potential and (B) time on the oxidation peak current of 10  $\mu\text{M}$  BPA in 0.1 M PBS (pH 8.0).

was then placed in an oil bath at 70 °C for 48 h. After cooling to room temperature, the condenser was washed with doubly distilled water and the sample solution was filtrated, and the filtrate was collected. Finally, doubly distilled water was added to make up 100 mL. A standard addition method was used to evaluate the analytical performance of the sensor. The results are shown in Table 1,

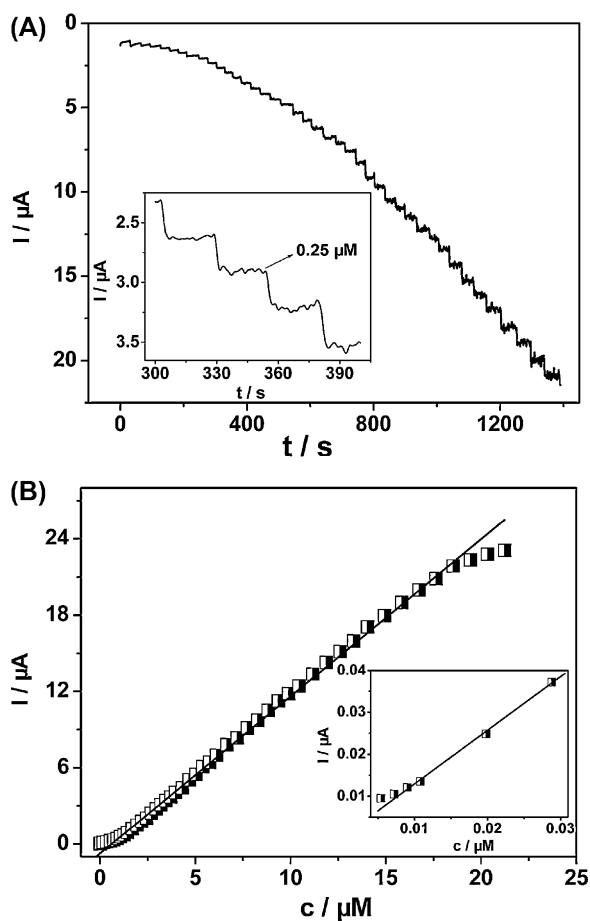


**Fig. 9.** (A) Current–time recording obtained at SWCNT-CD/GCE for the addition of 0.0054–21.2  $\mu\text{M}$  BPA into acutely stirred 0.1 M pH 8.0 PBS. Applied potential: 0.54 V. Inset: the magnification of 300–400 s. (B) Linear calibration curve. Inset: the magnification of 0.0054–0.03  $\mu\text{M}$ .

**Table 1**  
Determination of BPA in plastic samples.

Samples	Measured (nM) <sup>a</sup>	Added (nM)	Found (nM)	Recovery (%)
PC bottle	25.95	100	129.60	102.90
PC water bucket	36.54	100	130.90	95.86
PVC food package bag	53.23	100	149.39	97.49
PC baby bottle	13.52	100	116.33	102.47
PVC bottle	29.05	100	133.12	103.15

<sup>a</sup> Mean of five measurements.

and the recoveries are in the range of 95–103%, indicating that the sensor might be sufficient for practical applications.

## 5. Conclusion

Covalent functionalization of oxidized SWCNTs with amide-modified  $\beta$ -CD was accomplished by amidation reaction. The resultant  $\beta$ -CD-nanotube conjugate (SWCNT-CD) can be dispersed in water, and a stable and homogeneous SWCNT-CD film could be obtained after the suspension was cast onto the surface of GCE. Due to the excellent electrocatalytic properties of SWCNTs as well as the inclusion ability of  $\beta$ -CD to BPA, the SWCNT-CD modified GCE exhibited enhanced performance on the oxidation of BPA, improving its oxidation peak current, lowering its oxidation potential, and lowering detection limit for BPA (1.0 nM at S/N ratio of 3). The proposed method was successfully applied in determining BPA in real plastic samples with recovery ranging from 95% to 103%.

Additionally, the fabricated SWCNT-CD/GCE showed remarkable stability and reproducibility. Compared with other electrochemical methods, this new method possesses higher sensitivity and faster response.

## Acknowledgments

Financial support from Program for NSFC (51072172), International Joint Research Program of Hunan Province (2010WK2009), Key Project of Chinese Ministry of Education (209086), Scientific Research Fund of Hunan Provincial Education Department (08B085), and Open Project Program of Key Laboratory of Advanced Functional Polymeric Materials of Hunan Province (AFPM200904) is greatly acknowledged.

## References

- [1] A.C. Gore, Endocrine-disrupting Chemicals: From Basic Research to Clinical Practice, Humana Press Inc., New Jersey, 2007.
- [2] I.A. Lang, T.S. Galloway, A. Scarlett, W.E. Henley, M. Depledge, R.B. Wallace, D. Melzer, Association of urinary bisphenol A concentration with medical disorders and laboratory abnormalities in adults, *J. Am. Med. Assoc.* 300 (2008) 303–310.
- [3] A.M. Soto, C. Sonnenschein, Environmental causes of cancer: endocrine disruptors as carcinogens, *Nat. Rev. Endocrinol.* 6 (2010) 363–370.
- [4] A. Goodson, W. Summerfield, I. Cooper, Survey of bisphenol A and bisphenol F in canned foods, *Food Addit. Contam.* 19 (2002) 796–802.
- [5] L. Egan, Canada declares BPA toxic, sets stage for more bans. <http://www.theglobeandmail.com/news/national/canada-first-to-declare-bisphenol-a-toxic/article1755272/>.
- [6] J. Sajiki, K. Takahashi, J. Yonekubo, Sensitive method for the determination of bisphenol-A in serum using two systems of high-performance liquid chromatography, *J. Chromatogr. B* 736 (1999) 255–261.
- [7] H. Sambe, K. Hoshina, K. Hosoya, J. Haginaka, Direct injection analysis of bisphenol A in serum by combination of isotope imprinting with liquid chromatography–mass spectrometry, *Analyst* 130 (2005) 38–40.
- [8] J. Zhang, G.M. Cooke, I.H.A. Curran, C.G. Goodyer, X.-L. Cao, GC-MS analysis of bisphenol A in human placental and fetal liver samples, *J. Chromatogr. B* 879 (2011) 209–214.
- [9] A. Ballesteros-Gómez, S. Rubio, D. Pérez-Bendito, Analytical methods for the determination of bisphenol A in food, *J. Chromatogr. A* 1216 (2009) 449–469.
- [10] K. Ouchi, S. Watanabe, Measurement of bisphenol A in human urine using liquid chromatography with multi-channel coulometric electrochemical detection, *J. Chromatogr. B* 780 (2002) 365–370.
- [11] M.P. Zhao, Y.Z. Li, Z.Q. Guo, X.X. Zhang, W.B. Chang, A new competitive enzyme-linked immunosorbent assay (ELISA) for determination of estrogenic bisphenols, *Talanta* 57 (2002) 1205–1210.
- [12] H. Kuramitz, M. Matsushita, S. Tanaka, Electrochemical removal of bisphenol A based on the anodic polymerization using a column type carbon fiber electrode, *Water Res.* 38 (2004) 2331–2338.
- [13] H. Yin, Y. Zhou, S. Ai, R. Han, T. Tang, L. Zhu, Electrochemical behavior of bisphenol A at glassy carbon electrode modified with gold nanoparticles, silk fibroin, and PAMAM dendrimers, *Microchim. Acta* 170 (2010) 99–105.
- [14] V. Chauke, F. Matamadombo, T. Nyokong, Remarkable sensitivity for detection of bisphenol A on a gold electrode modified with nickel tetraamino phthalocyanine containing Ni–O–Ni bridges, *J. Hazard. Mater.* 178 (2010) 180–186.
- [15] H. Yin, L. Cui, S. Ai, H. Fan, L. Zhu, Electrochemical determination of bisphenol A at Mg–Al–CO<sub>3</sub> layered double hydroxide modified glassy carbon electrode, *Electrochim. Acta* 55 (2010) 603–610.
- [16] H. Yin, Y. Zhou, L. Cui, X. Liu, S. Ai, L. Zhu, Electrochemical oxidation behavior of bisphenol A at surfactant/layered double hydroxide modified glassy carbon electrode and its determination, *J. Solid State Electrochem.* 15 (2011) 167–173.
- [17] R.S.J. Alkassir, M. Ganesana, Y.H. Won, L. Stanciu, S. Andreescu, Enzyme functionalized nanoparticles for electrochemical biosensors: a comparative study with applications for the detection of bisphenol A, *Biosens. Bioelectron.* 26 (2010) 43–49.
- [18] P. Perez, R. Pulgar, F. Olea-Serrano, M. Villalobos, A. Rivas, M. Metzler, V. Pedraza, N. Olea, The estrogenicity of bisphenol A-related diphenylalkanes with various substituents at the central carbon and the hydroxy groups, *Environ. Health Perspect.* 106 (1998) 167.
- [19] C.R. Raj, T. Ohsaka, Electroanalysis of ascorbate and dopamine at a gold electrode modified with a positively charged self-assembled monolayer, *J. Electroanal. Chem.* 496 (2001) 44–49.
- [20] M.Y. Hua, H.C. Chen, R.Y. Tsai, Y.C. Lin, L. Wang, A novel biosensing mechanism based on a poly(N-butyl benzimidazole)-modified gold electrode for the detection of hydrogen peroxide, *Anal. Chim. Acta* 693 (2011) 114–120.
- [21] E. Spain, R. Kojima, R.B. Kaner, G.G. Wallace, J. O'Grady, K. Lacey, T. Barry, T.E. Keyes, R.J. Forster, High sensitivity DNA detection using gold nanoparticle functionalized polyaniline nanofibres, *Biosens. Bioelectron.* 26 (2011) 2613–2618.

- [22] D. Vega, L. Agüí, A. González-Cortés, P. Yáñez-Sedeño, J.M. Pingarrón, Electrochemical detection of phenolic estrogenic compounds at carbon nanotube-modified electrodes, *Talanta* 71 (2007) 1031–1038.
- [23] X. Tang, Y. Liu, H. Hou, T. You, A nonenzymatic sensor for xanthine based on electrospun carbon nanofibers modified electrode, *Talanta* 83 (2011) 1410–1414.
- [24] J. Wang, M. Musameh, Y. Lin, Solubilization of carbon nanotubes by nafion toward the preparation of amperometric biosensors, *J. Am. Chem. Soc.* 125 (2003) 2408–2409.
- [25] W. Wu, H. Zhu, L. Fan, D. Liu, R. Renneberg, S. Yang, Sensitive dopamine recognition by boronic acid functionalized multi-walled carbon nanotubes, *Chem. Commun.* (2007) 2345–2347.
- [26] M. Yang, Y. Yang, H. Yang, G. Shen, R. Yu, Layer-by-layer self-assembled multilayer films of carbon nanotubes and platinum nanoparticles with polyelectrolyte for the fabrication of biosensors, *Biomaterials* 27 (2006) 246–255.
- [27] Y.E. Shih, R.J. Jeng, Biodegradable poly (butylene succinate)/multi-walled carbon nanotube nanocomposites, in: V. Mittal (Ed.), *Nanocomposites with Biodegradable Polymers: Synthesis, Properties, and Future Perspectives*, Oxford University Press Inc., New York, 2011, pp. 101–122.
- [28] X. Tu, L. Yan, X. Luo, S. Luo, Q. Xie, Electroanalysis of bisphenol A at a multi-walled carbon nanotubes-gold nanoparticles modified glassy carbon electrode, *Electroanalysis* 21 (2009) 2491–2494.
- [29] J. Li, D. Kuang, Y. Feng, F. Zhang, M. Liu, Voltammetric determination of bisphenol A in food package by a glassy carbon electrode modified with carboxylated multi-walled carbon nanotubes, *Microchim. Acta* 172 (2011) 379–386.
- [30] J. Szejtli, Introduction and general overview of cyclodextrin chemistry, *Chem. Rev.* 98 (1998) 1743–1754.
- [31] K. Hanna, C. de Brauer, P. Germain, Cyclodextrin-enhanced solubilization of pentachlorophenol in water, *J. Environ. Manage.* 71 (2004) 1–8.
- [32] M.L. Singleton, J.H. Reibenspies, M.Y. Darensbourg, A cyclodextrin host/guest approach to a hydrogenase active site biomimetic cavity, *J. Am. Chem. Soc.* 132 (2010) 8870–8871.
- [33] Y. Domi, K. Ikeura, K. Okamura, K. Shimazu, M.D. Porter, Strong inclusion of inorganic anions into  $\beta$ -Cyclodextrin immobilized to gold electrode, *Langmuir* 27 (2011) 10580–10586.
- [34] H. Kitano, Y. Taira, Inclusion of bisphenols by a self-assembled monolayer of thiolated cyclodextrin on a gold electrode, *Langmuir* 18 (2002) 5835–5840.
- [35] H. Endo, T. Nakaji-Hirabayashi, S. Morokoshi, M. Gemmei-Ide, H. Kitano, Orientational effect of surface-confined cyclodextrin on the inclusion of bisphenols, *Langmuir* 21 (2005) 1314–1321.
- [36] R.C. Petter, J.S. Salek, C.T. Sikorski, G. Kumaravel, F.T. Lin, Cooperative binding by aggregated mono-6-(alkylamino)- $\beta$ -cyclodextrins, *J. Am. Chem. Soc.* 112 (1990) 3860–3868.
- [37] Y.Y. Liu, X.D. Fan, L. Gao, Synthesis and characterization of  $\beta$ -Cyclodextrin based functional monomers and its copolymers with N-isopropylacrylamide, *Macromol. Biosci.* 3 (2003) 715–719.
- [38] R. Ehret, W. Baumann, M. Brischwein, A. Schwinde, K. Stegbauer, B. Wolf, Monitoring of cellular behaviour by impedance measurements on interdigitated electrode structures, *Biosens. Bioelectron.* 12 (1997) 29–41.
- [39] P. Ajayan, Nanotubes from carbon, *Chem. Rev.* 99 (1999) 1787–1800.
- [40] C.E. Banks, A. Crossley, C. Salter, S.J. Wilkins, R.G. Compton, Carbon nanotubes contain metal impurities which are responsible for the “electrocatalysis” seen at some nanotube-modified electrodes, *Angew. Chem. Int. Ed.* 45 (2006) 2533–2537.
- [41] X. Dai, G.G. Wildgoose, R.G. Compton, Apparent ‘electrocatalytic’ activity of multiwalled carbon nanotubes in the detection of the anaesthetic halothane: occluded copper nanoparticles, *Analyst* 131 (2006) 901–906.
- [42] B. Šljukić, C.E. Banks, R.G. Compton, Iron oxide particles are the active sites for hydrogen peroxide sensing at multiwalled carbon nanotube modified electrodes, *Nano Lett.* 6 (2006) 1556–1558.
- [43] M. Murugananthan, S. Yoshihara, T. Rakuma, T. Shirakashi, Mineralization of bisphenol A (BPA) by anodic oxidation with boron-doped diamond (BDD) electrode, *J. Hazard. Mater.* 154 (2008) 213–220.
- [44] H. Kuramitz, Y. Nakata, M. Kawasaki, S. Tanaka, Electrochemical oxidation of bisphenol A. Application to the removal of bisphenol A using a carbon fiber electrode, *Chemosphere* 45 (2001) 37–43.
- [45] A.J. Bard, L.R. Faulkner, *Electrochemical Methods: Fundamentals and Applications*, second ed., Wiley, New York, 1980.
- [46] G. Wang, F. Wu, X. Zhang, M. Luo, N. Deng, Enhanced TiO<sub>2</sub> photocatalytic degradation of bisphenol A by  $\beta$ -cyclodextrin in suspended solutions, *J. Photochem. Photobiol. A: Chem.* 179 (2006) 49–56.
- [47] E. Laviron, Adsorption, autoinhibition and autocatalysis in polarography and in linear potential sweep voltammetry, *J. Electroanal. Chem.* 52 (1974) 355–393.
- [48] J.G. Velasco, Determination of standard rate constants for electrochemical irreversible processes from linear sweep voltammograms, *Electroanalysis* 9 (1997) 880–882.
- [49] F. Anson, Application of potentiostatic current integration to the study of the adsorption of cobalt (III)-(ethylenedinitrilo)tetraacetate on mercury electrodes, *Anal. Chem.* 36 (1964) 932–934.
- [50] I. Streeter, G.G. Wildgoose, L. Shao, R.G. Compton, Cyclic voltammetry on electrode surfaces covered with porous layers: an analysis of electron transfer kinetics at single-walled carbon nanotube modified electrodes, *Sens. Actuators B* 133 (2008) 462–466.
- [51] M.J. Sims, N.V. Rees, E.J.F. Dickinson, R.G. Compton, Effects of thin-layer diffusion in the electrochemical detection of nicotine on basal plane pyrolytic graphite (BPPG) electrodes modified with layers of multi-walled carbon nanotubes (MWCNT-BPPG), *Sens. Actuators B* 144 (2010) 153–158.
- [52] Y.D. Zhao, W.D. Zhang, H. Chen, Q.M. Luo, Anodic oxidation of hydrazine at carbon nanotube powder microelectrode and its detection, *Talanta* 58 (2002) 529–534.
- [53] S. Majidi, A. Jabbari, H. Heli, H. Yadegari, A. Moosavi-Movahedi, S. Haghgoo, Electrochemical oxidation and determination of ceftriaxone on a glassy carbon and carbon-nanotube-modified glassy carbon electrodes, *J. Solid State Electrochem.* 13 (2009) 407–416.
- [54] H. Yadegari, A. Jabbari, H. Heli, A. Moosavi-Movahedi, K. Karimian, A. Khodadadi, Electrochemical oxidation of deferiprone and its determination on a carbon nanotube-modified glassy carbon electrode, *Electrochim. Acta* 53 (2008) 2907–2916.
- [55] I. Streeter, L. Xiao, G.G. Wildgoose, G. Richard, Gold nanoparticle-modified carbon nanotubes-modified electrodes. using voltammetry to measure the total length of the nanotubes, *J. Phys. Chem. C* 112 (2008) 1933–1937.